This article was downloaded by: [National Chiao Tung University 國立交通大學]
On: 27 April 2014, At: 17:18
Publisher: Taylor & Francis
Informa Ltd Registered in England and Wales Registered Number: 1072954 Registered office: Mortimer House, 37-41 Mortimer Street, London W1T 3JH, UK

Aerosol Science and Technology
Publication details, including instructions for authors and subscription information:
http://www.tandfonline.com/loi/uast20

A Universal Calibration Curve for the TSI Aerodynamic Particle Sizer

Chuen-Jinn Tsai [a] , Sheng-Chieh Chen [a] , Cheng-Hsiung Huang [b] & Da-Ren Chen [c]
[a] Institute of Environmental Engineering, National Chiao Tung University , Hsin Chu, Taiwan
[b] Department of Environmental Engineering and Health, Yuanpei University of Science and Technology , Hsin Chu, Taiwan
[c] Department of Mechanical Engineering, Joint Program in Environmental Engineering, University of Washington in St. Louis , St. Louis, Missouri
Published online: 17 Aug 2010.

To cite this article: Chuen-Jinn Tsai , Sheng-Chieh Chen , Cheng-Hsiung Huang & Da-Ren Chen (2004) A Universal Calibration Curve for the TSI Aerodynamic Particle Sizer, Aerosol Science and Technology, 38:5, 467-474, DOI: 10.1080/02786820490460725

To link to this article: http://dx.doi.org/10.1080/02786820490460725

PLEASE SCROLL DOWN FOR ARTICLE

Taylor & Francis makes every effort to ensure the accuracy of all the information (the “Content”) contained in the publications on our platform. However, Taylor & Francis, our agents, and our licensors make no representations or warranties whatsoever as to the accuracy, completeness, or suitability for any purpose of the Content. Any opinions and views expressed in this publication are the opinions and views of the authors, and are not the views of or endorsed by Taylor & Francis. The accuracy of the Content should not be relied upon and should be independently verified with primary sources of information. Taylor and Francis shall not be liable for any losses, actions, claims, proceedings, demands, costs, expenses, damages, and other liabilities whatsoever or howsoever caused arising directly or indirectly in connection with, in relation to or arising out of the use of the Content.

This article may be used for research, teaching, and private study purposes. Any substantial or systematic reproduction, redistribution, reselling, loan, sub-licensing, systematic supply, or distribution in any form to anyone is expressly forbidden. Terms & Conditions of access and use can be found at http://www.tandfonline.com/page/terms-and-conditions

Aerosol Science and Technology, 38:467–474, 2004
Copyright © American Association for Aerosol Research
ISSN: 0278-6826 print / 1521-7388 online
DOI: 10.1080/02786820490460725

A Universal Calibration Curve for the TSI Aerodynamic Particle Sizer

Chuen-Jinn Tsai,[1] Sheng-Chieh Chen,[1] Cheng-Hsiung Huang,[2] and Da-Ren Chen[3]
[1]*Institute of Environmental Engineering, National Chiao Tung University, Hsin Chu, Taiwan*
[2]*Department of Environmental Engineering and Health, Yuanpei University of Science and Technology, Hsin Chu, Taiwan*
[3]*Department of Mechanical Engineering, Joint Program in Environmental Engineering, University of Washington in St. Louis, St. Louis, Missouri*

Downloaded by [National Chiao Tung University] at 17:18 27 April 2014

A universal calibration curve for the accurate determination of particle aerodynamic diameter by the TSI APS (TSI, Inc., St. Paul, MN, USA) operating at various temperature, pressure, particle, and gas properties is proposed. The previous dimensionless APS response function proposed by Chen et al. (1985) uses the Stokes number as the governing parameter and is valid in the Stokesian regime only. In the non-Stokesian regime, an additional non-Stokesian correction factor is needed to correct for the indicated aerodynamic diameters of the APS. The universal curve in the present study is based on the relationship between V_p^* and Stm, where $V_p^* = V_p/V_g$ and V_p is particle velocity, V_g is gas velocity at the nozzle exit, and Stm is modified Stokes number. Stm incorporates the non-Stokesian effect and is defined as 24St/(Re*C_D), where Re is the flow Reynolds number and C_D is the particle drag coefficient. We find that the new calibration curve can predict the particle aerodynamic diameter accurately within 6% of error under different operating conditions and particle/gas properties from the referenced condition without the need to introduce additional correction factors.

INTRODUCTION

The Aerodynamic Particle Sizer (APS, TSI, Inc., St. Paul, MN, USA) was developed to determine the aerodynamic diameter of airborne particles with high resolution. The instrument measures the transit time of a particle between two laser beams downstream of an accelerating nozzle. Due to the sudden acceleration of carrying gas at the nozzle exit, particles with larger inertia will lag more behind the accelerating gas stream and travel more slowly than particles of smaller inertia. Therefore, the particle transit time between two laser beams can be used to measure the particle aerodynamic diameter. The particle transit time, t, can be expressed as

$$t = \frac{L}{V_p}, \qquad [1]$$

where L and V_p are the distance and particle mean velocity between two laser beams, respectively. The particle transit time (with the unit of 10^{-9} s) is related to the APS channel N as (Rader et al. 1990)

$$t = (4N - 2). \qquad [2]$$

That is, the response of the APS can be expressed as the relationship between the channel number or particle velocity V_p versus the aerodynamic diameter. Due to physical variations among different APS units, a factory calibration is performed on each instrument before shipment. The APS response function depends primarily on Stokes number. However, a secondary effect on particle Reynolds number due to non-Stokesian effect will give rise to different APS responses (Wilson and Liu 1980; Rader et al. 1990). Rader et al. (1990) reviewed the previous literature on the effects of particle density on APS responses (Wilson and Liu 1980; Baron 1986; Ananth and Wilson 1988), as well as the methods to correct APS responses for particle density for spherical particles (Wang and John 1987, 1989) and nonspherical particles (Brockmann and Rader 1990). For large liquid particles, additional uncertainties in APS responses resulting from droplet deformation were found (Baron 1986; Brockmann et al. 1988; Tsai et al. 1998).

In an effort to find a unique APS response function, Chen et al. (1985) calibrated the APS at different sets of conditions. Their results showed that a unique calibration curve resulted for each APS when Stokes number, St, was plotted against V_p^* ($V_p^* = V_p/V_g$, where V_p is particle velocity, and V_g is gas velocity at

Received 1 July 2003; accepted 18 March 2004.
The authors would like to thank Dr. D. J. Rader and Dr. B. T. Chen for providing the original data of their experiments. Financial support of this work is provided by Taiwan NSC 89-2211-E-009-064.
Address correspondence to Chuen-Jinn Tsai, Institute of Environmental Engineering, National Chiao Tung University, No. 75 Poai Street, Hsin Chu, 300 Taiwan. E-mail: cjtsai@mail.nctu.edu.tw

Downloaded by [National Chiao Tung University] at 17:18 27 April 2014

the nozzle exit). The Stokes number, St, is defined as

$$\mathrm{St} = \frac{\rho_p D_p^2 V_g C}{9\mu_g W}, \qquad [3]$$

where

$$V_g = \left[\frac{2RT}{M_{\mathrm{air}}} \times \ln\left(\frac{P}{P - \Delta P}\right)\right]^{1/2}. \qquad [4]$$

In Equations (3) and (4), ρ_p, D_p, C, μ_g, W, R, T, M_{air}, P, and ΔP are the particle density (kg/m^3), particle diameter (m), slip correction factor for the particle of diameter D_p, gas viscosity ($\mathrm{N \cdot s/m^2}$), diameter of the nozzle at the exit (m), universal gas constant (8.3143 J/mol $\cdot$ K), operating ambient temperature (K), molecular weight of the air (28.9 g/mol), ambient pressure (mmHg), and pressure drop across the nozzle (mmHg), respectively.

The above universal APS response function is applicable in most cases. However, if the particle density is greater than 2000 kg/m^3, Wang and John (1987) found particle density affected the APS measurement. This density dependence of APS measurements was first pointed out by Wilson and Liu (1980) and was experimentally investigated by Baron (1984). In order to correct for the particle density effect, Wang and John (1987) developed a correction factor using the one-dimensional equation of motion for spherical particle in the non-Stokesian regime (Fuchs 1964). They found that the correction could be as large as 40% and 30% for $\rho_p = 200$ and 8000 kg/m^3, respectively, for a 20 μm particle diameter.

Rader et al. (1990) found that the dimensionless APS response function suggested by Chen et al. (1985) could be used up to a certain intermediate Stokes number with only reasonably small errors. However, due to non-Stokesian drag effect, large and systematic deviations from the reference (factory) calibration were observed for large values of Stokes number, particularly for the calibration in argon. The sizing errors amount to $<$12% for a nominal PSL diameter of 20 μm. A non-Stokesian correction factor had to be introduced to reduce the errors of measurement. Similar to Wang and John (1987), they derived another correction factor taking into account different gas properties at operating and reference calibration conditions as

$$F = \frac{\sqrt{\mathrm{St}_2^*}}{\sqrt{\mathrm{St}_1^*}} = \left(\frac{6 + R_2^{2/3}}{6 + R_1^{2/3}}\right)^{1/2}, \qquad [5]$$

where

$$R_i = \xi_i^{3/2}\sqrt{\mathrm{St}_i^*}|V_g - V_p|$$

$$\xi_i = \left(\frac{18\rho_{gi}^2 L}{\rho_{pi}\mu_{gi} V_g}\right)^{1/3}$$

The subscript 1 denotes properties (gas and particle) at the reference (calibration) condition, while the subscript 2 denotes properties (gas and particle) at the operating condition. The only unknown in Equation (5), $\sqrt{\mathrm{St}_2^*}$, can be obtained by iteration. St* is defined as

$$\mathrm{St}^* = \frac{\rho_p D_p^2 V_g C}{18\mu_g L},$$

where the slip correction factor C is evaluated at the downstream pressure of the nozzle. The derivation of Equation (5) requires that V_g is the same for both calibration and operating conditions, a so-called single-velocity mode of operation (Rader et al. 1990). This new correction factor reduces the differences between the argon calibration and the reference air calibration by about half.

Re-examination of the response function proposed by Chen et al. (1985) and subsequently by other investigators indicates that the Stokes number used in the function restricts its validity in the Stokesian regime only. This explains why the errors of measurement increase with an increasing Stokes number and why an additional correction factor has to be used to correct for the non-Stokesian effect. That is, a two-step procedure is needed to correct for the non-Stokesian effect, which could be due to the increase in particle density, particle diameter, and carrying gas flow rate, and change in operating temperature, pressure, and gas properties. It is desirable to have a universal calibration curve that incorporates the non-Stokesian effect in the governing parameters of the curve, so that an additional correction factor is not necessary. This can be achieved by using a modified Stokes number, which is based on the particle Stokes number, flow Reynolds number, and particle drag coefficient, as the governing parameter in the universal calibration curve.

UNIVERSAL CALIBRATION CURVE

The universal calibration curve proposed in this study is modified from the particle equation of motion described by Wilson and Liu (1980). In the dimensionless form, the equation of particle motion from the nozzle exit to the detecting laser beams can be express as

$$\frac{dV_p^*}{dt^*} = \frac{\mathrm{Re}(1 - V_p^*)^2 C_D}{24(\mathrm{St})}, \qquad [6]$$

where t^* is the dimensionless transit time. Reynolds number (Re) and drag coefficient (C_D) (Willeke and Baron 1993) are defined as

$$\mathrm{Re} = \frac{\rho_g V_g D_p}{\mu_g}, \qquad [7]$$

$$\begin{aligned} C_D &= \frac{24}{\mathrm{Re}_p}, \quad \mathrm{Re}_p < 0.1 \\ &= \frac{24}{\mathrm{Re}_p}(1 + 0.0916\mathrm{Re}_p), \quad 0.1 \le \mathrm{Re}_p < 5 \\ &= \frac{24}{\mathrm{Re}_p}\left(1 + 0.158\mathrm{Re}_p^{2/3}\right), \quad 5 \le \mathrm{Re}_p < 1000, \end{aligned} \qquad [8]$$

Downloaded by [National Chiao Tung University] at 17:18 27 April 2014

where particle Reynolds number in Equation (8), Re_p, is defined as

$$\mathrm{Re}_p = \frac{\rho_g (V_g - V_p) D_p}{\mu_g}. \quad [9]$$

Note that in the previous derivation of correction factors by Wang and John (1987) and Rader et al. (1990) the drag coefficient is only valid for $\mathrm{Re}_p \geq 5.0$.

From Equation (6), it is seen that V_p^* depends on the dimensionless parameters St, Re, and C_D only, and so should the APS responses. If one defines a modified Stokes number, Stm, as

$$\mathrm{Stm} = \frac{24\mathrm{St}}{\mathrm{Re} * C_D}, \quad [10]$$

then V_p^* depends solely on Stm only. That is, the APS response function described by the calibration curve of V_p^* versus Stm should be universal.

We used the experimental data of Chen et al. (1985) for the S/N 145 APS (TSI model 3300), Rader et al. (1990) for the S/N 311 and 106 APSs (TSI model 3300), and our own data for the S/N 431 APS (TSI model 3310A) to generate three different universal calibration curves based on one of these investigators' operating condition using air as the carrying gas. Each calibration curve was checked for accuracy against the experimental data of each investigator at other conditions/carrying gases. The experimental data of the APS S/N 145 were obtained by using 3 different total flow rates for different material particles with different densities (Chen et al. 1985). Besides polystyrene latex (PSL) particles, two kinds of liquid particles, dioctyl phthalate (DOP) and oleic acid (OA), were also used in the study by Chen et al. (1985). However, it was observed that liquid particles distorted into oblate spheroids in the acceleration field of the APS, resulting in underestimation of particle aerodynamic diameter (Willeke and Baron 1993). The droplet distortion appears to be a function of droplet viscosity and surface tension (Griffiths et al. 1986), and the shift in droplet diameter, Δ, can be corrected by an empirical equation (Baron et al. 2003) as

$$\Delta = a d_p^2 / (\sigma^b \mu^c), \quad [11]$$

where a, b, and c are fitted constants and σ is surface tension of the droplet (N/s). This droplet distortion effect was not considered in the unique calibration curve by Chen et al. (1985).

The APS S/N 311 and S/N 106 data were obtained by using different total flow rates and different carrying gases (air and argon) to sample PSL particles (Rader et al. 1990). Finally, our data for the APS S/N 431 were obtained under three different total flow rates by using PSL particles.

To further validate the accuracy of the proposed universal calibration curve, the effects of particle density, operating pressure, and temperature on the APS responses, new correction factors were calculated by fixing Stm at both reference calibration and operating conditions. These correction factors were then compared with those calculated by Rader et al. (1990). Although we show later that the differences in the correction factors by the two methods are very small, it is to be noted that the correction factors are not needed once the universal calibration curve developed in this study is adopted.

The particle slip correction factor, carrying gas density, and viscosity are dependent on the downstream pressure and temperature of the nozzle. We assumed one-dimensional isentropic ideal gas flow at the nozzle exit because the Mach numbers are always greater than 0.3 for the APS. Gas properties at the nozzle exit can be found by Equations (11)–(14) as (Fox and McDonald 1985):

$$\frac{\rho_{g0}}{\rho_g} = \left[1 + \frac{K-1}{2} M^2\right]^{1/K-1}, \quad [12]$$

$$\frac{P_0}{P} = \left[1 + \frac{K-1}{2} M^2\right]^{K/K-1}, \quad [13]$$

$$\frac{T_0}{T} = 1 + \frac{K-1}{2} M^2, \quad [14]$$

$$M = \frac{V_g}{\sqrt{KRT/M_{\mathrm{gas}}}}, \quad [15]$$

where ρ_{g0}, P_0, and T_0 are stagnation (ambient conditions) gas density, pressure, and temperature, respectively; ρ_g, P, and T are the corresponding properties at any arbitrary position (downstream of the nozzle); and K and M_{gas} are the specific heat ratio of gas (for air $K = 1.4$) and gas molecular weight, respectively. Substituting Equation (15) into Equation (13), the relationship between V_g and P can be expressed as

$$\left(\frac{P - \Delta P}{P}\right)^{\frac{1-K}{K}} = 1 + \frac{(K-1) V_g^2 M_{\mathrm{gas}}}{2KRT}. \quad [16]$$

This equation is different from Equation (4), which assumes isothermal condition at the nozzle exit. From this equation, and Equations (12) and (14) the actual gas density, viscosity, and temperature downstream of the nozzle can be obtained and used in establishing the universal calibration curves and computing the new correction factors.

RESULTS AND DISCUSSION

Comparing the Present Universal Calibration Curves with the Calibration Curves of Chen et al. (1985)

Figures 1 to 3 compare the present universal calibration curves with the experimental data at different conditions and the calibration curves suggested by Chen et al. (1985). In these figures, instead of plotting V_p^* versus St (or Stm), we plot St (or Stm) versus V_p^* to facilitate the use of the calibration curves to calculate the aerodynamic diameter from the APS responses. Figure 1a is the experimental data obtained in this study plotted as St versus V_p^*, following the method by Chen et al. (1985), at three different total flow rates (Q_t) for PSL particles (APS S/N

Downloaded by [National Chiao Tung University] at 17:18 27 April 2014

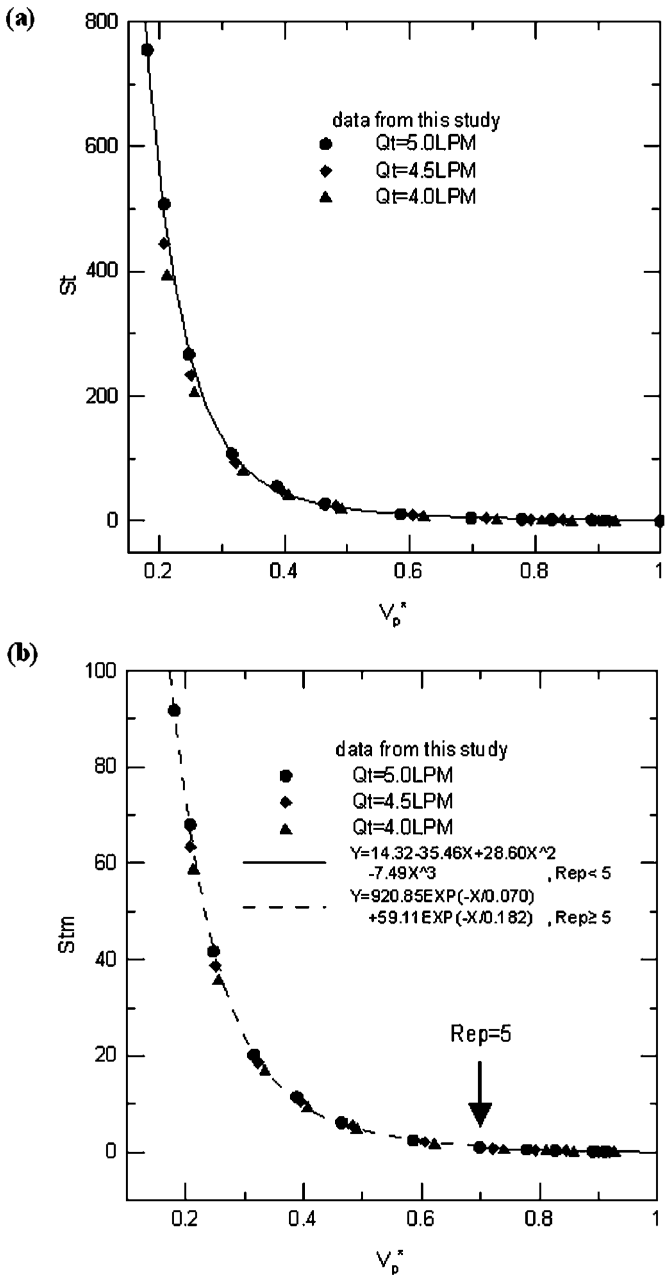

Figure 1. (a) Calibration curve plotted as V_p^* versus St. (b) Present universal calibration curve plotted as V_p^* versus Stm. Curves are for the data at $Q_t = 5.0$LPM. Experimental data from the present study, APS S/N 431.

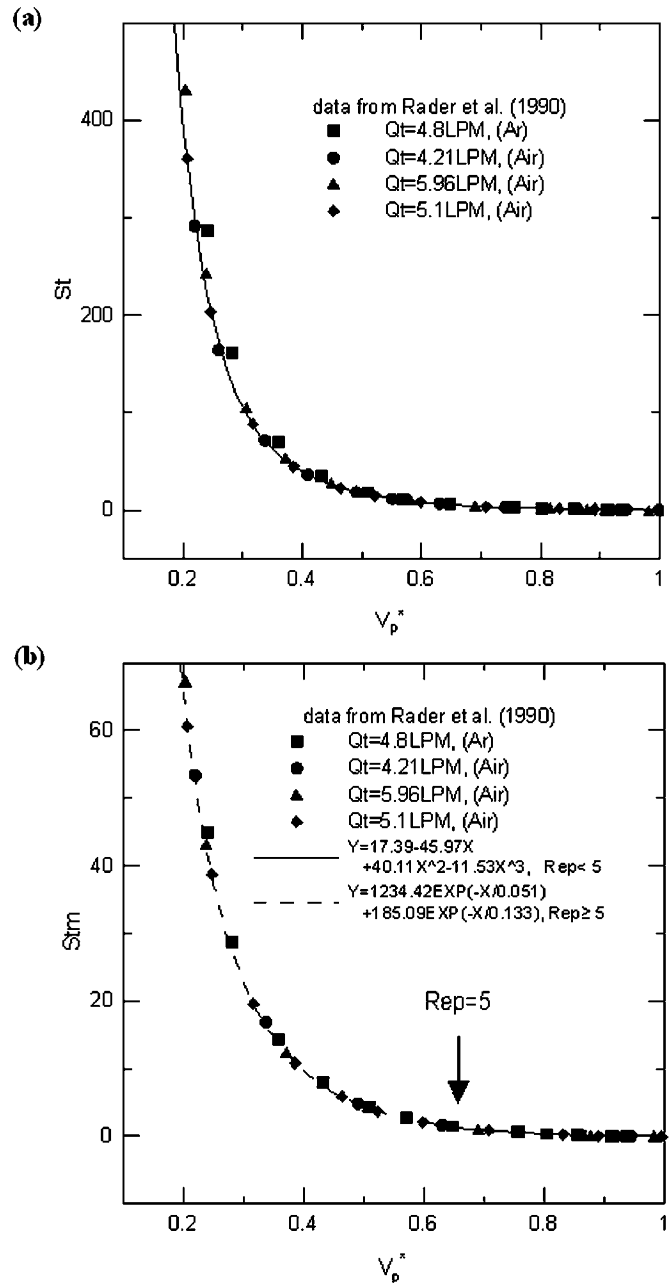

Figure 2. (a) Calibration curve plotted as V_p^* versus St. (b) Present universal calibration curve plotted as V_p^* versus Stm. Curves are for the data at $Q_t = 5.1$LPM. Experimental data from Rader et al. (1990), APS S/N 311.

431). It is seen that three data sets fall in the same calibration curve when St < 100, but some data points begin to deviate from the curve when St > 100 due to non-Stokesian effects. The deviation increases with an increasing St. For example, for the same 21.4 μm PSL particles, the deviation of St for $Q_t = 5$LPM and $Q_t = 4$LPM is the maximum and is 22.3%, corresponding to an uncertainty in the aerodynamic diameter of about 10%. The calibration curve is plotted by using the experimental data at $Q_t = 5$LPM. If the curve is established using the data set at other flow rates, similar deviation at large St is found. In comparison, the universal calibration curve shown in Figure 1b, which is obtained by substituting Stm for St in the y axis, indicates that all experimental data almost fall on the same universal calibrating curve obtained at $Q_t = 5$LPM. The maximum deviation of Stm for $Q_t = 5$LPM and $Q_t = 4$LPM is reduced to 12.6% for 21.4 μm particles, corresponding to a maximum uncertainty in

Downloaded by [National Chiao Tung University] at 17:18 27 April 2014

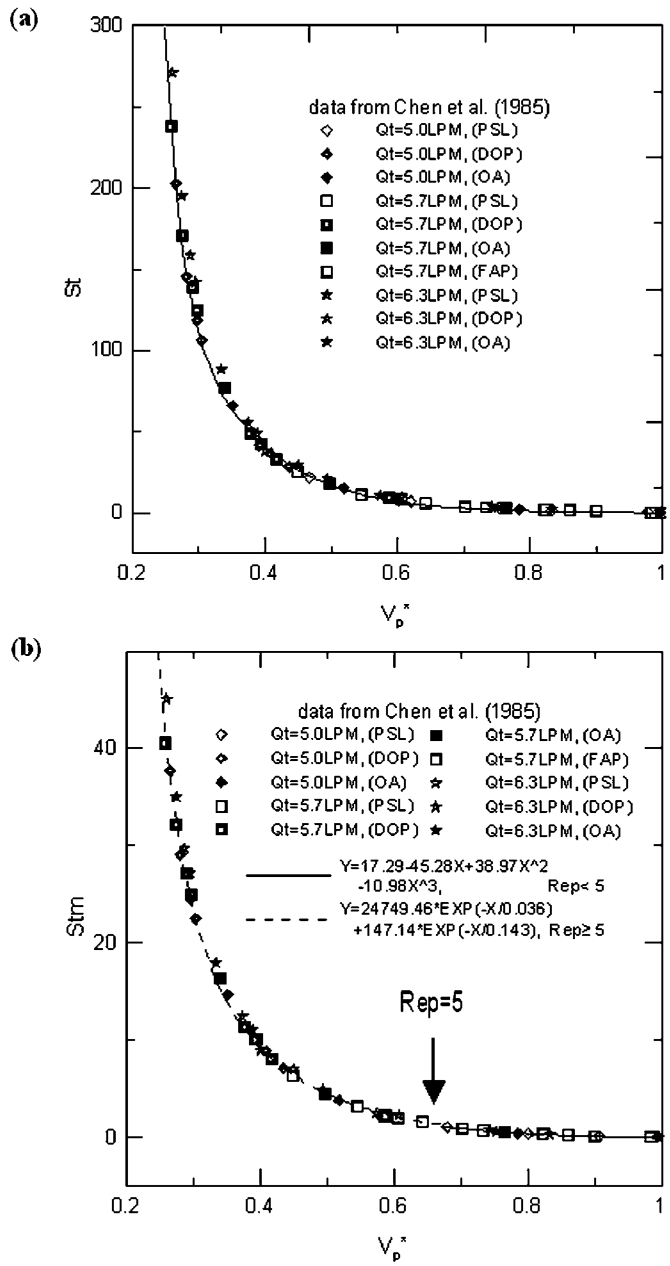

Figure 3. (a) Calibration curve plotted as V_p^* versus St. (b) Present universal calibration curve plotted as V_p^* versus Stm. Curves are for the data at $Q_t = 5.0$LPM. Experimental data from Chen et al. (1985), APS S/N 145.

aerodynamic diameter of about 4.8%. Similar errors were found when the universal calibration curve was established using flow rates other than 5LPM.

The fitted equations for the universal calibration curves in Figure 1b, and subsequently in Figures 2b and 3b, are obtained by the least-square regression using the polynomial function for $0.1 \leqq \text{Rep} < 5$ and the exponential decay function of the second-order for $5 \leqq \text{Rep} < 1000$ based on the experimental data at $Q_t = 5$LPM. It is found that no single function can fit all experimental data over the entire range of Rep.

Similarly, Figures 2 and 3 show better agreement of the universal calibration curve with the experimental data by Rader et al. (1990) and Chen et al. (1985), respectively. Larger deviation from the experimental data was found when the traditional calibration curve was plotted as St versus V_p^*. For example, in Figure 2a the deviation is the maximum for 20 μm particles carried by argon, which is 26% in St, corresponding to an uncertainty in the aerodynamic diameter of about 12%, which was also described in Rader et al. (1990). Based on the experimental data at $Q_t = 5.1$LPM using air as the carrying gas, the universal calibration curve of the APS S/N 311 is able to predict the aerodynamic diameter for the APS operating at different flow rates and carrying gases to within 4.5% accuracy (Figure 2b). That is, the universal calibration curve established using the current method at a certain reference calibration not only can predict the particle aerodynamic diameter at other operating flow rates but also with different carrying gases.

Chen et al. (1985) used three different total flow rates to calibrate particles of different materials (PSL particles in the size range between 0.2 and 5 μm, OA or DOP particles between 1.5 and 16 μm, and fused aluminosilicate particles (FAP) particles between 0.5 and 4 μm) for the APS S/N 145. The particle densities were 0.894, 0.986, 1.00–1.05, and 2.3 g/cm^3 for OA, DOP, PSL, and FAP, respectively. Again, the traditional calibration curve of St versus V_p^* deviates more from the experimental data than the universal calibration curve (Stm versus V_p^*), as shown in Figure 3. The universal curve is again shown to predict the particle aerodynamic diameter accurately with the maximum error of 6% (occurs for 16 μm DOP particles) for such a wide range of flow rates and particle densities. In comparison, the maximum error using the traditional calibration curve by Chen et al. (1985) is 9.9% (also occurs for the 16 μm DOP particles).

If the distortion of OA and DOP particles was considered, and the particle diameter due to droplet distortion effects was adjusted by Equation (11) (Baron et al. 2003) to establish another unique calibration curve, it was found that the maximum error of predicting the aerodynamic diameter did not reduce. Instead of the maximum error of 9.9%, it became 11.2% for the 16 μm DOP droplets. Similarly, for the present universal calibration curve considering droplet distortion effect, the accuracy was not improved either. One of the possible reasons is that the gas velocity change (or flow rate change) was not considered in Equation (11).

That is, for a maximum sizing error of <6%, once the universal calibration curve is established at a certain reference calibration condition for an APS, the same curve can be used at different flow rates, carrying gases, temperatures, pressures, and particle densities. There is no need to recalibrate the APS, and the use of correction factors is not necessary either.

To use the universal calibration curve at a particular operating condition, V_p^* is first calculated from a certain indicated channel number and total operating flow rate (or V_g). From the universal curve, Stm can be found and the corresponding aerodynamic diameter can then be calculated. Iteration is needed since C_D depends on Rep.

To check if the three universal calibration curves, represented by Figures 1b, 2b, and 3b, for three different APSs are different, these curves were plotted on the same graph. Results showed that the maximum differences between the curves are <10% in terms of the aerodynamic diameter. This error is about twice as much as that of the individual calibration curve. This indicates the need to calibrate each APS individually to avoid uncertainties due to physical variations.

In conclusion, the main idea of the universal calibration curve is to have the curve built on one set of conditions that can then be applied to all other conditions. The procedure of building the curve is as follows:

1. Calibrate the APS under a particular condition using solid particles (such as PSL) to obtain the relationship of channel number versus actual aerodynamic diameter.
2. Calculate Stm and the corresponding V_p^* by Equations (1)–(3), (7)–(8), and (12)–(15).
3. Fit the value (V_p^* versus Stm) by polynomial regression for $0.1 \leqq \text{Rep} < 5$ and exponential decay function of the second order for $5 \leqq \text{Rep} < 1000$.

Effects of Particle Density, Carrying Gas, and Operating Pressure and Temperature

The previous investigators used a two-step method to correct for the aerodynamic diameter indicated by the APS. Here it is demonstrated that the current universal calibration curve can also be used to generate the same correction factors as the previous investigators, although these correction factors are not really needed when the universal curve is adopted to calculate the actual aerodynamic diameter under a particular operating condition. In the last section, it is demonstrated that each APS responded uniquely to a single parameter, Stm. As long as Stm is the same between two conditions, the indicated APS aerodynamic diameter should be the same but can be different from the actual aerodynamic diameter. For calculating the correction factor, the single-velocity mode of operation was used. The correction factor was defined as the ratio of the actual aerodynamic diameter to the indicated aerodynamic diameter.

Figure 4 shows the comparison of the effect of particle density on the correction factors between the present method and the method of Rader et al. (1990); see Equation (5). Good agreement is seen between these two methods. The particle density effect increases (and the correction factor deviates more from 1.0) with an increasing particle diameter and increasing deviation from unit particle density. The correction factor will approach 0.7 for $\rho_p = 8000$ kg/m^3 and 1.10 for $\rho_p = 500$ kg/m^3 at the channel number 875 (corresponding to the aerodynamic diameter of 26.1 μm). Small difference between the two methods is observed when the particle density deviates too much from the density of the calibrating particles, $\rho_{pc} = 1050$ kg/m^3, and the maximum difference of 0.9% occurs at the channel number

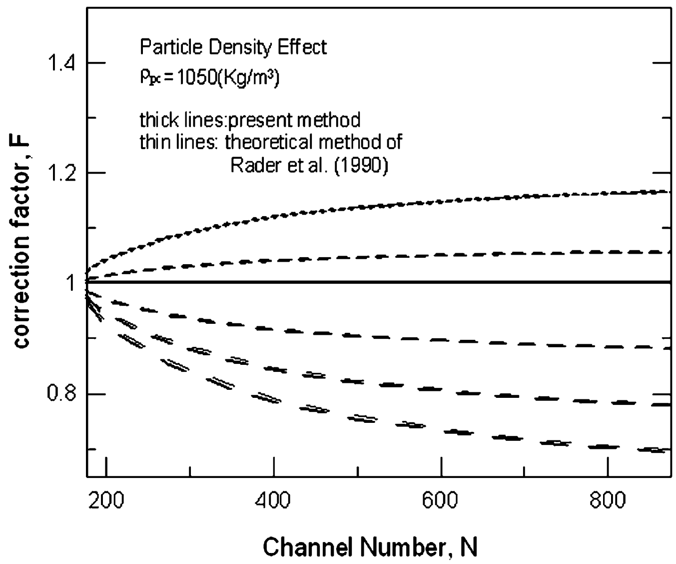

Figure 4. Correction factor versus channel number, different particle densities (fixed $T = 293$ K, $P = 760$ mmHg).

875 for $\rho_p = 8000$ kg/m^3. In contrast to the isothermal assumption adopted by Rader et al. (1990) and previous investigators, the current correction factors were calculated based on the gas properties assuming isentropic flow (see Equations (12) to (14)). These two different assumptions result in differences in downstream temperature of 15 K and gas velocity of 2.5 m/s, and they contribute to a maximum difference of 0.5% in the collection factors in the channel 875 between the two methods. Other difference in the correction factors is caused by different methods used to calculate the correction factors.

Baron's experimental data (filled symbols) (1986) were also used to check if the current method can correct for the particle density effect to obtain actual aerodynamic diameters from the APS's indicated aerodynamic diameters. Potassium biphthalate (KHP) and sodium tungstate (N_aWO_4), with densities ranging from 1100–1190 and 2000–2500 kg/m^3, respectively, were used in Baron's experiment. Figure 5 shows that the calibration curve obtained using PSL particles gives indicated aerodynamic diameters that are higher than the actual diameters (represented by filled symbols in Figure 5). Without correction, the maximum error of prediction by the calibration curve obtained using PSL particles can be as much as 12%. The current method can obtain accurate aerodynamic diameters (represented by open symbols) with a maximum error of less than 3.9%.

Figure 6 shows the correction factors due to operating pressure effects. When the operating pressure is less than the calibration pressure at 760 mmHg, the correction factor is less than 1.0 and decreases with a decreasing pressure. The correction factor is about 0.85 if P = 500 mmHg at the channel number 875. The correction factors by the present method and Rader et al. (1990) are very close to each other, with the maximum difference of <0.9% for all particle sizes (channel numbers).

Downloaded by [National Chiao Tung University] at 17:18 27 April 2014

Downloaded by [National Chiao Tung University] at 17:18 27 April 2014

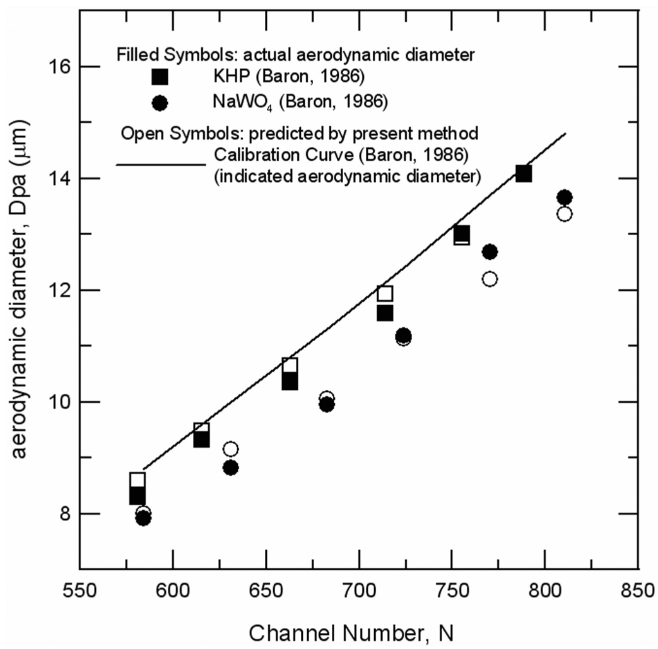

Figure 5. Comparison of calibration curve generated by PSL particles with APS response at two different particle densities. Filled symbols, experimental data by Baron (1986); open symbols, predicted by the present method.

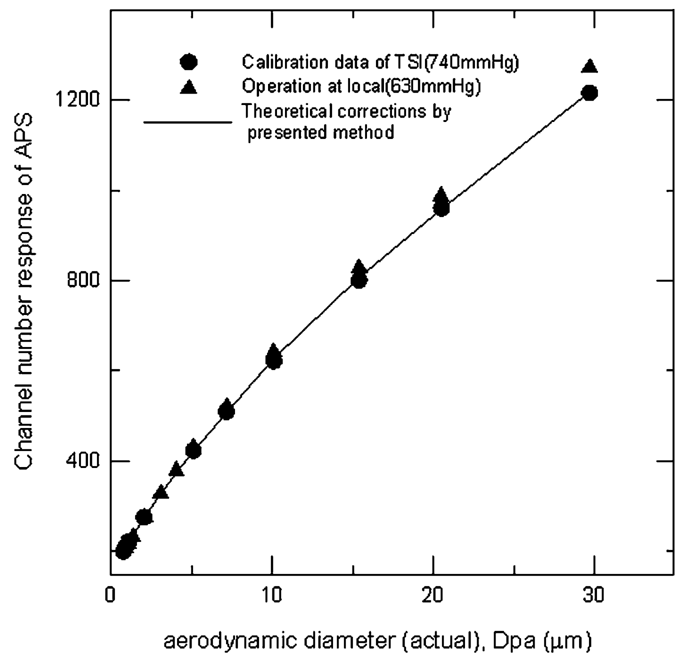

Figure 7. Channel response for the APS S/N 106 operated at two different ambient pressures. Solid curve is the corrected response at 740 mmHg by the present method based on TSI's calibration at 630 mmHg.

Figure 7 shows the differences in the APS (S/N 106) responses between the TSI calibration at $P = 740$ mmHg and $T = 293$ K, and that of Rader et al. (1990) at $P = 630$ mmHg and $T = 295$ K, using the same V_g. The deviation in the channel number is large for large particles, and the maximum is about 4.7% for 29.0 μm particle. Using the prediction by the present method at $P = 630$ mmHg and $T = 295$ K, the maximum deviation from the TSI calibration for the channel number is down to 0.3% (corresponding to an uncertainty in aerodynamic diameter of <1%).

The operating temperature effect on the correction factors is shown in Figure 8 in the temperature range of 265–325 K. The correction factor is not significantly different from 1.0 and is within 1 ± 0.04 for all particle sizes. The correction factors of the two methods differ by at most 4.2% at 325 K, channel number 875.

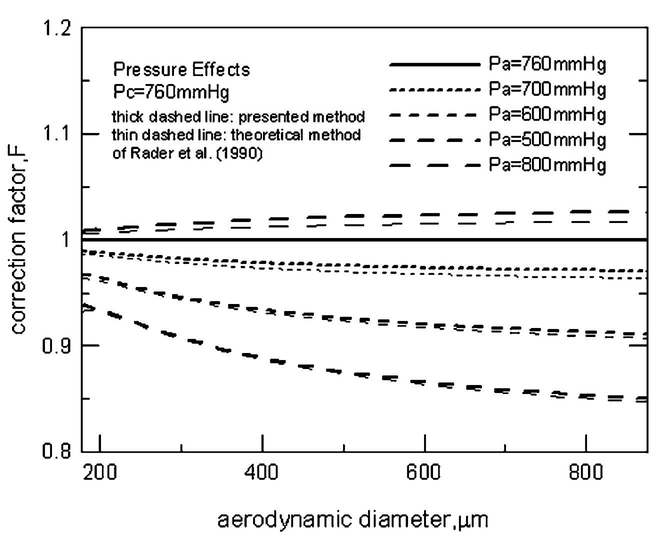

Figure 6. Correction factor versus channel number at various operating pressures (fixed $T = 293$ K).

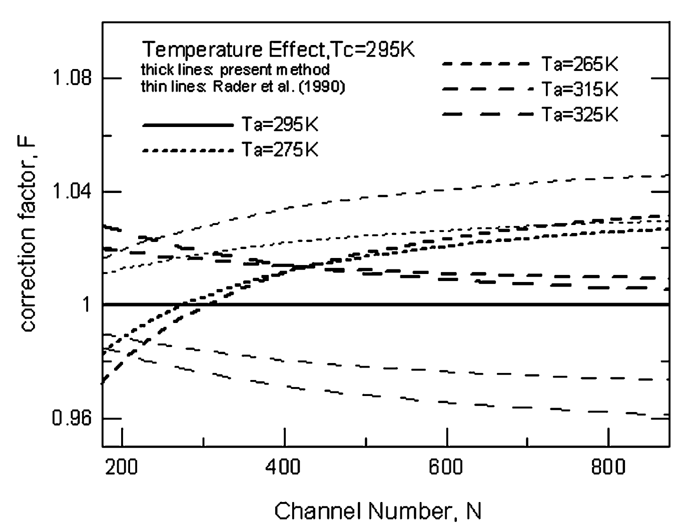

Figure 8. Correction factor versus channel number at various operating temperatures (fixed $P = 1$ atm).

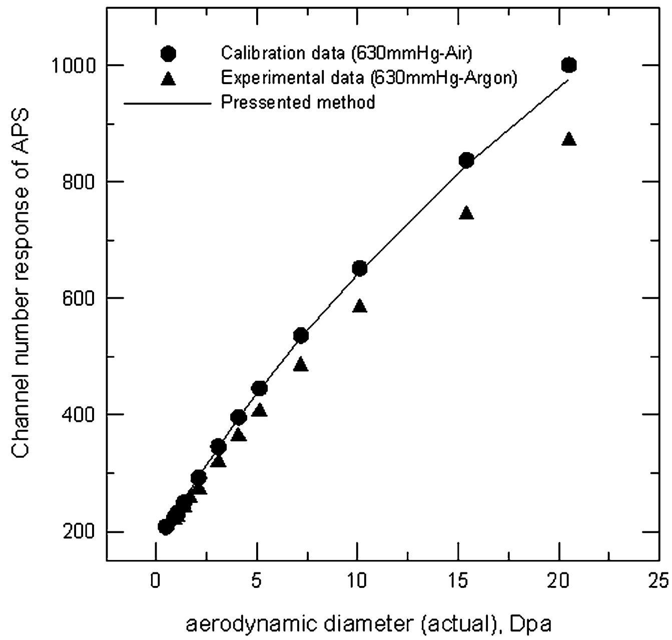

Figure 9. Channel response for the APS S/N 311 calibrated with air and argon (experimental data by Rader et al. 1990). Solid curve is the corrected response for argon by the present method based on the reference calibration by air.

The present method can be used to correct for the APS responses when operating the APS in a carrying gas other than air, which is normally used in the reference calibration. As shown in Figure 9, the channel number response is quite different for the air and argon calibration data (Rader et al. 1990). The difference in the channel number increases with an increasing diameter, and is 12.5% for a 20 μm particle. After correcting by the present method, the difference in the channel number is reduced to 2.3% for a 20 μm particle, corresponding to an uncertainty in aerodynamic diameter of about 3.8%.

CONCLUSIONS

The responses of the APS are influenced by the non-Stokesian effect, and the indicated particle aerodynamic diameters must be corrected for particle density, flow rate, gas properties, operating pressure, and temperature if the operating condition is different from the reference calibration. This study has demonstrated that a universal calibration curve can be obtained at a reference calibration and applied to other operating conditions and carrying gases to obtain accurate aerodynamic diameters with less than 6% of errors without recalibration. The assumption of single-velocity mode of operation is not necessary. Using a modified Stokes number, $\text{Stm} = 24\text{St}/(\text{Re} * C_D)$, the non-Stokesian effect embedded in the flow Reynolds number, Re, and drag coefficient, C_D, is automatically incorporated in the universal calibration curve. The accuracy of the universal calibration curves has been confirmed by the experimental data of previous investigators and the present experiment at different flow rates, particle densities, carrying gases, and operating pressures.

The effects of particle density, operating pressure, and temperature on the correction factors have been studied by the present method and are compared with those by the method of Rader et al. (1990). In general, good agreement is obtained. In summary, if the current universal calibration is used to establish the APS responses, these correction factors are not needed, and recalibration of the APS at a particular operating condition is unnecessary unless extreme accuracy is desired.

This study used calibration data obtained by earlier models of the APS. It is worthwhile to study the calibration data of the new TSI model 3321 APS in the future. Also, to complete the calibration study of the APS, a more accurate equation should be developed to predict the distortion effect of the droplets on the underestimation of aerodynamic diameter, as suggested by Baron et al. (2003).

REFERENCES

Ananth, G., and Wilson, J. C. (1988). Theoretical Analysis of the TSI Aerodynamic Particle Sizer, *Aerosol Sci. Technol.* 9:189–199.

Baron, P. A. (1984). In *Aerosols*, edited by B. Y. H. Liu, D. Y. H. Pui, and H. J. Fissan. Elsevier, New York, pp. 215–216.

Baron, P. A. (1986). Calibration and Use of the Aerodynamic Particle Sizer (APS 3300), *Aerosol Sci. Technol.* 5:55–67.

Baron, P. A., Anthony B. M., and Erica N. J. (2003). Correction of Droplet Distortion Effects. In *Aerodynamic Particle Sizing Instruments*, AAAR, Anaheim, California, 20–24 October, p. 141.

Brockmann, J. E., Yamano, N., and Lucero, D. (1988). Calibration of the Aerodynamic Particle Sizer 3310 (APS-3310) with Polystyrene Latex Monodisperse Spheres and Oleic Acid Monodisperse Particles, *Aerosol Sci. Technol.* 8:279–281.

Brockmann, J. E., and Rader, D. J. (1990). APS Response to Nonspherical Particles and Experimental Determination of Dynamic Shape Factor, *Aerosol Sci. Technol.* 13:162–172.

Chen, B. T., Cheng, Y. S., and Yeh, H. C. (1985). Performance of a TSI Aerodynamic Particle Sizer, *Aerosol Sci. Technol.* 4:89–97.

Fox, R. W., and McDonald, A. T. (1985). *Introduction to Fluid Mechanics,* John Wiley & Sons, New York, pp. 577–579.

Fuchs, N. A. (1964). *The Mechanics of Aerosols*, Pregamon Press, Oxford.

Griffiths, W. D., Iles, P. J., and Vaughan, N. P. (1986). The Behaviour of Liquid Droplet Aerosols in an APS 3300, *J. Aerosol Sci.* 17:921–930.

Rader, D. J., Brockmann, J. E., Ceman, D. L., and Lucerto, D. A. (1990). A Method to Employ the Aerodynamic Particle Size Factory Calibration under Different Operating Conditions. *Aerosol Sci. Technol.* 13:514–521.

Tsai, C. J., Chein, H. M., Chang, S. T., and Kuo, J. Y. (1998). Performance Evaluation of an API Aerosizer, *J. Aerosol Sci.* 29:839–853.

Wang, H.-C., and John, W. (1987). Particle Density Correction for Aerodynamic Particle Sizer, *Aerosol Sci. Technol.* 6:191–198.

Wang, H.-C., and John, W. (1989). A Simple Iteration Procedure to Correct for the Density Effect in the Aerodynamic Particle Sizer, *Aerosol Sci. Technol.* 10:501–505.

Willeke, K., and Baron, P. A. (1993). *Aerosol Measurement,* Van Nostrand Reinhold, New York, pp. 30–31.

Wilson, J. C., and Liu, B. Y. H. (1980). Aerodynamic Particle Size Measurement by Laser-Doppler Velocimetry. *J. Aerosol Sci.* 11:139–150.

Downloaded by [National Chiao Tung University] at 17:18 27 April 2014